Infrared multiphoton photochemistry of hexafluorobenzene studied by time-resolved visible luminescence spectroscopy

ARTICLE *in* THE JOURNAL OF PHYSICAL CHEMISTRY · OCTOBER 1983

Impact Factor: 2.78 · DOI: 10.1021/j100245a015

3 AUTHORS, INCLUDING:

Shammai Speiser
Technion - Israel Institute of Technology
307 PUBLICATIONS **2,027** CITATIONS

To our knowledge, there are no previous results for CO or CO_2 hydrogenation in well-defined systems with poisons and promoters used at the same time. However, previous studies on Fe catalysts have shown that addition of K increases the resistance of the catalysts to S poisoning.[71,72] Our results show that CO formation proceeds in the presence of both K(a) and S(a) as if the S(a) were absent. As noted previously, the effect on CH_4 production seems to be a coverage-weighted average of the individual effects of S(a) and K(a). This supports the idea that the effects of S(a) and K(a), separately and together, reflect the changes of electron density in the metal rather than any direct, local-site effects, at least for CH_4 formation. Much more study, however, should be directed into this area to gain a better understanding of these processes.

V. Summary

The activation energy for CH_4 formation from CO_2 at total pressures of 97 and 120 torr over a Ni(100) single-crystal surface is 21.2 kcal mol^{-1}. The activation energy and absolute rates for CH_4 formation from CO_2 are very close to the values seen from CO under identical reaction conditions. Rapid formation of large amounts of CO was seen, with the activation energy for formation increasing from an initial value of 17.4 to a steady-state value of 19.7 kcal mol^{-1}. The results support a mechanism where CO_2 is converted to CO and then to C(a) before hydrogenation.

Preadsorption of K and/or S gives rise to no drastic changes in reaction mechanism. At $H_2/CO_2 = 96/1$ and a total pressure of 97 torr, the adsorption of K increases the rate of production of both CO and CH_4, affecting CO more strongly, but the overall activation energy is unchanged. The adsorption of S decreases the rate of production of both CO and CH_4, affecting CH_4 more strongly. The adsorption of both K and S shows that the K(a) can compensate for the effects of S(a). The production of CO is increased up to the level seen when K(a) is alone on the surface while the production of CH_4 reflects a coverage-weighted average of the individual effects of K(a) and S(a). This supports an electronic interaction model for the effects of S(a) and K(a), rather than local bonding effects.

Registry No. Carbon dioxide, 124-38-9; nickel, 7440-02-0; methane, 74-82-8; potassium ion, 24203-36-9; sulfur, 7704-34-9.

(72) R. B. Anderson, F. S. Karn, and J. F. Shultz, *J. Catal.*, 4, 56 (1965).

Infrared Multiphoton Photochemistry of Hexafluorobenzene Studied by Time-Resolved Visible Luminescence Spectroscopy[1a]

Michael T. Dulgnan,[1b] Ernest Grunwald,* and Shammai Speiser[1b]

Department of Chemistry, Brandeis University, Waltham, Massachusetts 02254 (Received: March 7, 1983)

C_6F_6 gas (0.15–3 torr) was irradiated with IR pulses at 1023 cm^{-1}, where C_6F_6 absorbs strongly, and the time evolution of the visible/near-UV luminescence spectrum was examined. IR pulse fluence ranged mostly from 100 to 900 J cm^{-2}, and square-pulse equivalent intensity from 2 to 18 GW cm^{-2}. By use of a plasma shutter to truncate IR pulses after ~60 ns, luminescence evolving during irradiation could be clearly distinguished from that emitted subsequently. Kinetic measurements at 360 nm showed that luminescence begins shortly (10–20 ns) after the start of the IR pulse. After pulse truncation, the initial decay of luminescence comprises two first-order lifetimes, $\tau_A \approx 15$ ns and $\tau_B = 575 \pm 75$ ns. Time-resolved spectroscopy shows that the 575-ns emission agrees closely with a well-characterized emission, previously assigned to C_3, seen in carbon furnaces and fuel-rich oxyacetylene flames. During the period 1.8–18.8 μs after the IR pulse, time-resolved spectra are dominated by broad-background emission, with sharp superposed intensity peaks assignable to C_2 Swan bands. The broad-background emission during this period agrees with blackbody radiation spectra for temperatures decreasing from 3640 to 3440 K. The luminescence yield for the background emission varies as the square of the initial C_6F_6 pressure. Final reaction products are mostly C_2F_4(g) and a black solid ("fluorocoal") of approximate composition $(C_2F)_n$. It is suggested that the final products indicate *not* how the parent molecules decompose but how the fragments formed from them reassemble afterward as the gas temperature returns to ambient.

Introduction

It was found early in the history of infrared laser chemistry with pulsed CO_2 lasers that at very high intensities, of the order of 10^9 W cm^{-2}, absorbing gas molecules decompose rapidly and small fragments appear, some of them in excited electronic states.[2,3] For example, irradiation with focused IR beams at appropriate wavenumbers produced SiF* from SiF_4 ($\Delta E > 460$ kcal mol^{-1}),[2,5] C_2* from C_2H_4 ($\Delta E > 240$ kcal mol^{-1}),[3,5] and CN*, C_2*, and CH* from CH_3CN.[3] In these experiments, the characteristic luminescence from the electronically excited

(1) (a) We thank the Edith C. Blum Foundation and the National Science Foundation for grants which provided partial support. (b) Present address: M.T.D., Code 6540, Naval Research Laboratory, Washington, DC 20375; S.S., Department of Chemistry, Technion-IIT, Haifa 32000 Israel.

(2) Isenor, N. R.; Merchant, V.; Hallsworth, R. S.; Richardson, M. C. *Can. J. Phys.* **1973**, *51*, 1281.

(3) Ambartzumian, R. V.; Chekalin, N. V.; Letokhov, V. S.; Ryabov, E. A.; *Chem. Phys. Lett.* **1975**, *36*, 301.

(4) (a) Bialkowski, S. E.; Guillory, W. A. *J. Chem. Phys.*, **1977**, *67*, 2061. (b) Lesiecki, M. L.; Guillory, W. A. *Ibid.* **1977**, *66*, 4317.

(5) Sources for thermochemical and spectroscopic data are the following: (a) "JANAF Thermochemical Tables", 2nd ed.; National Bureau of Standards: Washington, DC, 1971; *Natl. Stand. Ref. Data Ser. (U.S., Natl. Bur. Stand.)* No. 37, 1141 pages. (b) Huber, K. P.; Herzberg, G. "Constants of Diatomic Molecules"; Van Nostrand-Reinhold: Princeton, NJ, 1979; pp 112, 138, 140, 154. (c) Benson, S. W.; Cruickshank, F. R.; Golden, D. M.; Haugen, G. R.; O'Neal, H. E.; Rodgers, A. S.; Shaw, R.; Walsh, R. *Chem. Rev.* **1969**, *69*, 279.

0022-3654/83/2087-4387$01.50/0

fragments appeared in the focal region already during the IR pulse, in less than 150 ns after the start of irradiation.[2,3]

There are examples, also, in which the luminescent species are *not* simply fragments of the parent absorber. For instance, IR photolysis of CH_3OH under similar conditions yields not only such fragments as CH* and OH* but also dicarbon C_2*,[3,4] showing that at least some bimolecular reactions of the fragments are detectable on the 150-ns time scale of this experiment.[3] One may note, in this connection, that the process $2CH \rightarrow C_2^*(^3\pi_g) + H_2$ is exothermic.[5] Because of the high sensitivity of luminescence detection, the amount of C_2* formed may have been quite small.

The early experiments[2] on luminescence in SiF_4, due to SiF*, also illustrated two other phenomena. First, there is a time lag (called the *incubation period*[6]) between the start of the IR pulse and the appearance of luminescence. Second, relatively soon after the incubation period, an approximate dynamic steady state is reached in which the profile of SiF* luminescence vs. time closely follows that of laser intensity vs. time, even to the extent of responding to mode beats.[2] The time lag varies roughly as I^{-1}, where I is the intensity of the IR beam,[7] and (at constant I) represents[6,8] the mean time needed for the complex series of IR excitation and decomposition steps leading from SiF_4 to SiF* in the subsequent steady state. In the experiments described,[2] incubation periods ranged from 40 to 100 ns. In other cases, with other substrates, they are even shorter.[6,9]

Background Radiation. While luminescence spectra measured synchronously with the IR laser pulse show mostly the band structure characteristic of emission from small molecules, spectra of *total* luminescence per pulse often show such band structure superimposed on a broad emission background.[10] Evidently this type of luminescence is emitted mostly late in the pulse and after the pulse. The broad backgrounds from different substrates are similar to each other and bear a marked resemblance to blackbody radiation spectra.[11]

When a solid product appears, this emission could be due to nascent product particles suspended in the irradiated gas. When there is no solid product (and perhaps, generally, because of the high energy density produced in the IR-irradiated gases) the backgrounds could represent emission by free electrons, even though the IR excitation takes place under conditions which avoid dielectric breakdown and the gases do not become strongly ionized. Indeed, except for their low intensities and spectral distributions indicative of substantially lower temperatures, the backgrounds resemble the radiation emitted by electrons in hot plasmas.[12]

Probable Mechanism of Fragmentation. The evolution of luminescence as a function of time of course depends on the nature of the fragmentation reactions under the given conditions. For medium-sized substrate molecules, observations at lower intensities suggest the following picture.

1. Fragmentation is a series of decompositions rather than a concerted molecular fission. The initial scission of the parent molecules takes place in the electronic ground state and involves the same decomposition channels as do thermal reactions.[13] However, in contrast to thermal reactions, the mean energy of the decomposing molecules at high radiational pumping rates lies high above the reaction thresholds for the major decomposition channels,[14] so that polyatomic products tend to be formed at energy levels within their vibrational quasi-continua and therefore to absorb further[15] and to decompose further. This process of repeated IR absorption and decomposition will continue until either the radiation stops or the molecular fragments become so small that they are no longer formed in vibrational quasi-continua.

2. After the IR pulse is over, the gas contains a high proportion of small, energy-rich, and reactive molecules, some of them in excited electronic states. Judging by the broad emission backgrounds, temperatures might be in the 3000–4000 K range. The heat capacity of the gas is likely to be high because heat losses by physical cooling are compensated in part by heat inputs from chemical reactions as chemical equilibria approached at earlier times shift in accordance with Le Chatelier's principle. Observations in gases irradiated at lower IR intensities[16] suggest that high temperatures might persist for at least a few microseconds, which would be long enough for significant relaxation toward chemical equilibrium to occur. Let us therefore define a reference temperature $^\phi T$ on the basis of the broad-background emission, so that $^\phi T$ is the temperature of the blackbody radiation that gives statistical "best fit" to the background emission. Emission bands will then appear *superimposed on the background* if the ratio of populations of the emitting or upper state to that of the resulting or lower state is greater than the equilibrium ratio at $^\phi T$; absorption bands will appear if the ratio is smaller.

Reasons for Study of C_6F_6. Our reactant gas, hexafluorobenzene (C_6F_6), is a good substrate for the study of these complex phenomena. Not only is C_6F_6 a strong IR absorber, but at constant pulse fluence (F_p) the amount of radiant energy absorbed per mole (E_{abs}) is independent of pressure.[17,18] If this lack of pressure dependence holds at the much higher fluences used in the present experiments, it will facilitate the interpretation of kinetic measurements of luminescence as a function of pressure. The C_6F_6 molecules are medium-sized, large enough for irradiation at high intensities to produce a stepwise series of decompositions, if that is indeed the mechanism. The accompanying progressive changes in the nature of the UV/visible luminescing species should be observable by time-resolved spectroscopy. Emission spectra are known for a number of potential electronically excited interme-

(6) Yahav, G.; Haas, Y.; Carmeli, B.; Nitzan, A. *J. Chem. Phys.* **1980**, *72*, 3410.

(7) This relationship between intensity and incubation period should not be confused with the $I^{3/2}$ dependence often observed for luminescence or product yield in focused geometries. Speiser, S.; Jortner, J. *Chem. Phys. Lett.* **1976**, *44*, 3283.

(8) Quack, M. *J. Chem. Phys.* **1978**, *69*, 1282. (b) Quack, M. *Ber. Bunsenges. Phys. Chem.* **1979**, *83*, 757. (c) Quack, M.; Humbert, P.; Van den Bergh, H. *J. Chem. Phys.* **1980**, *73*, 247.

(9) (a) Stephenson, J. C.; King, D. S. *J. Chem. Phys.* **1978**, *69*, 1485. (b) Stephenson, J. C.; King, D. S.; Goodman, M. F.; Stone, J. *Ibid.* **1979**, *70*, 4496. (c) Stephenson, J. C. *Ibid.* **1982**, *77*, 3283.

(10) (a) Yu, M. H.; Reisler, H.; Mangir, M.; Wittig, C. *Chem. Phys. Lett.* **1979**, *62*, 439. (b) Burak, I.; Tsao, J. Y. *Ibid.* **1981**, *77*, 536. (c) Yahav, G.; Haas, Y. *Ibid.* **1981**, *83*, 493. (d) Lesiecki, M. L.; Guillory, W. A. *J. Chem. Phys.* **1977**, *66*, 4317.

(11) Kompa, K. L. "Proceedings of the 28th IUPAC Congress, Vancouver, British Columbia, Canada, 1981", paper PH179.

(12) Armstrong, B. H.; Nicholls, R. W. "Emission, Absorption, and Transfer of Radiation in Heated Atmospheres", Pergamon Press: Oxford, 1972.

(13) (a) Bloembergen, N.; Yablonovitch, E.; *Phys. Today* **1978**, *31* (May), 23. (b) Oref, I.; Rabinovitch, B. S. *Acc. Chem. Res.* **1979**, *12*, 166. (c) Danen, W. C. *Opt. Eng.* **1980**, *1*, 21.

(14) This is implied by all kinetic models. See, for example, ref 9c and ref 15.

(15) Duperrex, R.; Van den Bergh, H. *Chem. Phys.* **1979**, *40*, 275.

(16) (a) Speiser, S.; Grunwald, E. *Chem. Phys. Lett.* **1980**, *73*, 438. (b) Garcia, D.; Grunwald, E. *J. Am. Chem. Soc.* **1980**, *102*, 6407.

(17) $F_p = \int I\,dt$ for the given pulse. E_{abs}/F_p has the dimensions of cross section per mole and is anlogous to the molar extinction coefficient in Beer's law.

(18) Duignan, M. T.; Garcia, D.; Grunwald, E. *J. Am. Chem. Soc.* **1981**, *103*, 7281.

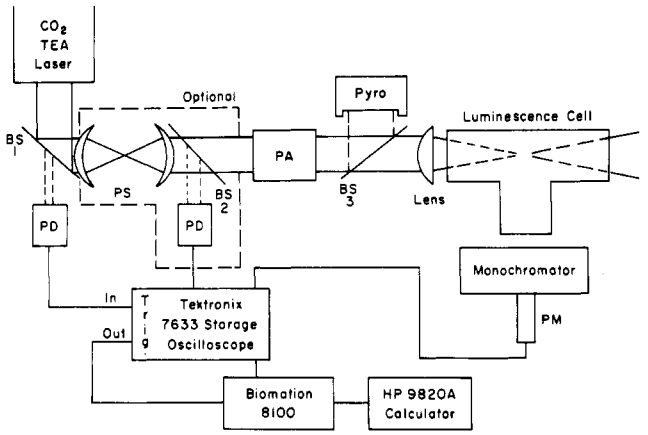

Figure 1. Diagram of fexperimental setup: (BS) beam splitters (No. 1, 95% reflecting; Nos. 2 and 3, 10% reflecting); (PD) photon drag detector, Rofin Model 7415, 1-ns response; (PA) polarizer–attenuator; (PS) plasma shutter; (Pyro) Lumonics Model 200 D pyroelectric meter; (Lens) 12.7-cm fl, ZnSe plano-convex.

diates, including C_6F_6*,[19] $C_6F_6^+$,[20] CF_2*,[21] CF*,[5b] C_3*,[22,23] and C_2*.[5b]

Among the emitting species formed early during the irradiation may be electronically excited parent molecules, C_6F_6*, formed in such processes as inverse electronic relaxation[24] or direct IR excitation[25] from vibrationally excited electronic ground-state molecules.

Visual Observations. When C_6F_6 (1 torr, in a glass cell with KCl windows) was irradiated at 1023 cm^{-1} with 1 J cm^{-2} pulses, there appeared within the cell at each laser pulse a cylinder of faint orange light of the same width as, and coincident with, the collimated IR beam. Increasing the fluence to 2 J cm^{-2} caused a brilliant orange luminescence clearly visible even in daylight. The area from which the orange light originated now appeared more diffuse but was brightest within the IR beam. Increasing sample pressure resulted in more light near the entrance window and less near the rear window. Decreasing the sample pressure to ~200 mtorr caused the entire cell volume (several times the beam volume) to glow with each laser pulse. Again, the brightest area came from within the beam. Increasing the fluence further (>20 J cm^{-2}) by focusing the IR beam changed the color of the luminescence to a whitish blue.

Present Work. In quantitative studies of these phenomena reported in this paper, we used time-resolved emission spectroscopy, scanning from 250 to 650 nm, at C_6F_6 pressures ranging from 0.2 to 4 torr. The full 1023-cm^{-1} IR pulses consisted of 120-ns "spikes" followed by ~1-μs "tails"; 95% of the pulse fluence was delivered in 800 ns. In some experiments we used a plasma shutter to truncate the IR pulses after ~60 ns[26a] to examine, for the first time, the decay kinetics of species present early after the start of irradiation. Time-resolved measurements of luminescence yields as functions of pressure enabled us to distinguish[27] between emitting species descended from parent C_6F_6 in unimolecular processes and those whose formation requires bimolecular collisions.

Experimental Part

Measuring System. A schematic diagram is shown in Figure 1. The CO_2 TEA laser is a Lumonics Model 103-1 and operated at 1023 cm^{-1} (P44 of 00°1–02°0 CO_2 transition). The IR pulse consisted of a 120-ns fwhm spike and an ~1-μs tail. Laser energy was monitored with a pyroelectric meter (Lumonics Model 200 D) and any laser energy drift was compensated by readjustment of the polarizer–attenuator. Laser energy was focused through polished KCl windows to the center of a 101 mm length × 25 mm diameter stainless steel cell by means of a 12.7 cm focal length $f/5$ plano-convex ZnSe lens. The beam waist in the focal region was approximated by a cylinder 1 cm in length and 0.2 mm in diameter. (The diameter was estimated by measuring the threshold energy at which 100-ns IR pulses focused by the ZnSe lens caused optical breakdown in air and using an intensity threshold of 1×10^9 W cm^{-2} for such breakdown.)

Luminescence was observed perpendicular to the beam axis. The monochromator/photomultiplier (PM) instrumentation varied (see below). The signals were amplified with a Tektronix 7A13 amplifier and then digitized with a Biomation Model 8100 wave-form recorder (8 bit × 2K channels, 10 ns/sample).

Hexafluorobenzene (Aldrich) was degassed and introduced into the stainless steel cell by standard vacuum-line techniques. Sample purity was checked by GC/MS (Poropak Q stationary phase) and was ~99.9%.

Luminescence Kinetics. Instead of a monochromator we used either a 360-nm interference filter (47% transmission, 10-nm fwhm) or a 560-nm interference filter (40% transmission, 6-nm fwhm). The PM was a side-looking EMI Model 9781 B with a measured response time of ~5 ns and an electron transit time of 40 ns (at 490 V) under the experimental conditions. Overall response time of the PM plus electronics (after allowance for the electron transit time) was ~12 ns.

A plasma shutter, whose construction is described elsewhere,[26a] was used to truncate the IR pulse to a width of 60 ns (measured at 10% of peak). Truncation was effectively complete in less than the instrumental response time. In this way we avoided difficulties encountered by other investigators when measuring decay rates while IR energy was still being deposited in the system.[27]

Most of the experiments were done with focused beams. Pulse fluence (F_p) ranged from ~100 to 900 J cm^{-2} in the focal region. Mean intensity at which the fluence was delivered ($I_f = F_p^{-1} \int I^2\, dt$)[18] ranged from ~2 to 18 GW cm^{-2}.

Time-Resolved Spectroscopy. An ISA Model H20 UV-1200 grating monochromator (resolution ~ 6 nm) allowed time-resolved UV/vis spectra to be taken. A wide spectral response PM (EMI 9798 QB; electron transit time ~90 ns at 590 V) was used, but overall system time re-

(19) (a) Al-Ani, K.; Philips, D. *J. Phys. Chem.* **1970**, *74*, 4046. Philips, D. *J. Chem. Phys.* **1967**, *46*, 4679. (b) O'Connor, D. B.; Sumitani, M.; Morris, J. M.; Yoshihara, K. *Chem. Phys. Lett.* **1982**, *93*, 350. (c) Loper, G. L.; Lee, E. K. C. *Ibid.* **1972**, *13*, 140. Our own measurements confirm these authors' spectrum of C_6F_6.

(20) (a) Bondybey, V. E.; English, J. H.; Miller, T. A. *J. Am. Chem. Soc.* **1978**, *100*, 5251; **1979**, *101*, 1248. (b) Allan, M.; Maier, J. P.; Marthaler, O. *Chem. Phys.* **1977**, *26*, 131.

(21) (a) Koda, S. *Chem. Phys. Lett.* **1978**, *55*, 353. (b) Hikida, T.; Tozawa, T.; Mori, Y. *Ibid.* **1980**, *70*, 579. (c) King, D. S.; Schenck, P. K.; Stephenson, J. C. *J. Mol. Spectrosc.* **1979**, *78*, 1. (d) Sheinson, R. S.; Toby, F. S.; Toby, S. *J. Am. Chem. Soc.* **1975**, *97*, 6593. (d) Barger, R. L.; Broida, H. P. *J. Chem. Phys.* **1965**, *43*, 2371.

(22) (a) Brewer, L.; Engelke, J. L. *J. Chem. Phys.* **1962**, *36*, 992. (b) Marr, G. V.; Nicholls, R. W. *Can. J. Phys.* **1955**, *33*, 394. (c) Marr, G. V. *Ibid.* **1957**, *35*, 1265. (d) Barger, R. L.; Broida, H. P.; *J. Chem. Phys.* **1965**, *43*, 2364.

(23) (a) Gausset, L.; Herzberg, G.; Lagerquist, A.; Rosen, B. *Astrophys. J.* **1965**, *142*, 45. (b) Becker, K. H.; Tatarczyk, T.; Radic-Peric, J. *Chem. Phys. Lett.* **1979**, *60*, 502.

(24) Nitzan, A.; Jortner, J. *J. Chem. Phys.* **1979**, *71*, 3524.

(25) Friedmann, H.; Kimel, S.; Schroder, H., private communication of unpublished results.

(26) (a) Duignan, M. T. Ph.D. Dissertation, Brandeis University, Waltham, MA, 1982; Chapter 1. (b) *Ibid.*, Chapter 3. See this chapter for details of calibration, control experiments, and additional plots of results.

(27) See, for example: Reisler, H.; Wittig, C. *Adv. Chem. Phys.* **1981**, *47*, 679.

sponse had to be increased to ~130 ns to maintain adequate signal/noise. Luminescence was measured from 250 to 650 nm. Nontruncated IR pulses were employed and F_p was ~1200 J cm^{-2} in the focal volume. The angle of light acceptance in the plane including the IR beam and perpendicular to the monochromator slit was ~20°, as viewed from the slit. The light detection system actually monitored a 2.5-cm segment of the IR beam including the ~1-cm beam waist. The luminescence signal was digitized by the Biomation Model 8100 wave-form recorder and integrated over the following *successive* time intervals: 0.3, 0.5, 1, 2, 5, and 10 μs. During the initial 0.3-μs interval, 80% of the pulse fluence is delivered. After the next interval (0.5 μs, 16% of pulse fluence), the IR pulse is essentially over, so the subsequent four intervals are after the IR pulse. Total observed time thus was 18.8 μs after the start of the IR pulse. C_6F_6 pressure was 1.26 ± 0.01 torr. Tests were performed[26b] to ensure that dielectric breakdown was not occurring.

Results and Discussion

Chemistry. When C_6F_6 was irradiated at 1023 cm^{-1} at a fluence of >1.5 J cm^{-2}, under conditions leading to visible luminescence, gaseous products observed by GC/mass spectral analysis were mostly C_2F_4, accompanied by small amounts of $CF_3C_6F_5$, C_3F_6, and C_4F_8 and by traces of CF_4 and C_2F_6. These products account for ~75% of the fluorine and somewhat less than 50% of the carbon of the depleted C_6F_6. Also formed was a black, sooty deposit which, for lack of a better name, will be called "fluorocoal". Mass balance suggests that this solid is carbon rich, of overall formula C_xF_y, where $x/y \approx 2$.

To avoid accumulation of a sooty deposit of fluorocoal on the optical windows, a focused geometry was used so that fluence at the windows was low and the reaction volume was small. Time between IR pulses exceeded 1 min, which appeared to be long enough for the solid particles to settle (vide infra) and the gaseous products to diffuse out of the reaction zone. C_2F_4 remained the principal gaseous product, up to the highest fluence below dielectric breakdown.[28]

The formation of C_2F_4 and of the minor products $CF_3C_6F_5$, C_3F_6, and C_4F_8 indicates that CF_2 is a reaction intermediate. This evidence for CF_2 from C_6F_6 is consistent with recent reports[29] that irradiation of C_6F_6 with a KrF laser also produces CF_2. Indeed, C_6F_6 is said to be an excellent source of CF_2 by this method.[29b]

Reactions and Energetics for C_6F_6 Decomposition. According to measured or estimated standard enthalpies of formation,[5] decomposition paths of lowest $\Delta H°$ are (1) C–F bond breaking,[30] (2) C–C bond breaking, and (3) a more complicated process involving *m*-fluorine migration coupled with retro-Diels–Alder decomposition.

$$C_6F_6 \xrightarrow{\Delta H° \approx 114 \text{ kcal}} C_6F_5\cdot + F\cdot \quad (1)$$

$$\xrightarrow{\Delta H° \approx 120 \text{ kcal}} \cdot CF{=}CF{-}CF{=}CF{-}CF{=}CF\cdot \quad (2)$$

$$\xrightarrow{\Delta H° \approx 114 \text{ kcal}} FC{\equiv}C{-}C{\equiv}CF + F_2C{=}CF_2 \quad (3)$$

For fluorine compounds, thermochemical estimates of $\Delta H°$ are relatively uncertain. Moreover, values of $\Delta H°$ for endothermic reactions at best define lower limits to reaction thresholds. In the present cases, the discrepancy is probably greatest for reaction 3. Thus, even though reaction 3 entails a low estimate for $\Delta H°$ and provides a plausible explanation for the principal reaction products, any of the three channels may be significant.

At high IR pumping rates, as stated earlier, reaction tends to occur from levels of vibrational excitation that lie well above the threshold energy. This effect is important to the reaction mechanism because it promotes further IR absorption and reaction. The magnitude of the effect tends to increase with molecular size. We now wish to estimate it for C_6F_6 at the present reaction conditions.

Let E_v denote vibrational energy of a molecule above the zero-point energy and assume, for definiteness, that there is a single reaction channel. Following common practice in IR multiphoton chemistry,[31] divide the E_v scale into energy shells based on the photon energy $h\nu_L$. A molecule is assigned to the *n*-th shell if $(n - {}^1/_2)h\nu_L < E_v < (n + {}^1/_2)h\nu_L$.

Let $k(n)$ denote the specific reaction rate for the population of the *n*-th energy shell. Let $c(n,I)$ denote the *n*-th shellwise concentration in the assumed steady state at intensity I, and let $r(n,I) = k(n)\ c(n,I)$ be the shellwise reaction rate. Let n_0 denote the shell number of the energy range that includes the reaction threshold.

As n increases above n_0, $k(n)$ increases, but $c(n,I)$ decreases progressively because in each energy shell above n_0 some substrate molecules disappear by reaction. The shellwise reaction rate $r(n,I) = k(n)\ c(n,I)$ therefore passes through a maximum at some particular value $n = n_R$. We shall refer to the n_R-th shell as the *most probable energy shell for reaction* in the steady state at the given intensity.

Let dn_{abs}/dt be the mean rate of absorption of IR photons. It can then be shown that n_R is related to dn_{abs}/dt and $k(n)$ according to expression 4. Thus, if $k(n)$

$$\left[\frac{1}{k(n_R-1)} - \frac{1}{k(n_R)}\right]^{-1} < \left[\frac{dn_{abs}}{dt}\right]_I < \left[\frac{1}{k(n_R)} - \frac{1}{k(n_R+1)}\right]^{-1} \quad (4)$$

can be estimated for the given reaction and dn_{abs}/dt is known, expression 4 will permit an estimate to be made of n_R.

In applying expression 4 to C_6F_6 we considered specifically C–F bond breaking, reaction 1, because the estimation of $k(n)$ by RRKM theory is then straightforward.[32] However, similar results would be expected for reactions 2 and 3, and indeed for unimolecular decomposition of any molecules of similar size.

The absorption law for C_6F_6 reported previously[18] had been tested up to $I = 1.2 \times 10^7$ W cm^{-2} at which $dn_{abs}/dt = 2.5 \times 10^8$ s^{-1}. Introducing this value in expression 4 one finds that $n_R = 87$ (1023 cm^{-1}) photons, or 140 kcal mol^{-1} above the threshold ($n_0 = 39$) for C–F bond breaking. This calculation establishes a lower limit because the actual mean intensity in our experiments is 3.6×10^9 W cm^{-2}, or

(28) (a) For UV emission and products resulting from dielectric breakdown of C_6F_6, see: Gilbert, R.; Theoret, A. *J. Phys. Chem.* **1976**, *80*, 1017. (b) By tuning the laser to ~1090 cm^{-1} (well away from the C_6F_6 absorption band) we observed a marked decrease in emission, even at substantially higher fluences than those used in the experiments at 1023 cm^{-1}. This would rule out dielectric breakdown as a source of the luminescence.

(29) (a) Dornhofer, G.; Hack, W.; Langel, W., presented at the 15th International Symposium on Free Radicals, June 2–7, 1981, Ingonish Beach, Nova Scotia, Canada, paper E7. (b) Langel, W., private communication.

(30) Okafo, E. N.; Whittle, E. *Int. J. Chem. Kinet.* **1978**, *10*, 591.

(31) Thiele, E.; Goodman, M. F.; Stone, J. *Opt. Eng.* **1980**, *19*, 10.

(32) (a) Normal-mode vibrations of C_6F_6 were taken from: Green, J. H. S.; Harrison, D. J. *J. Chem. Thermodyn.* **1976**, *8*, 529. (b) It was assumed that the 1493-cm^{-1} C–F stretch becomes unstable in the transition state for C–F bond breaking. (c) $k(n)$ was calculated according to RRKM theory, using the Whitten–Rabinovitch approximation for vibration-state densities and sums. Robinson, P. J.; Holbrook, K. J. "Unimolecular Reactions"; Wiley: New York, 1972; Chapter 5.

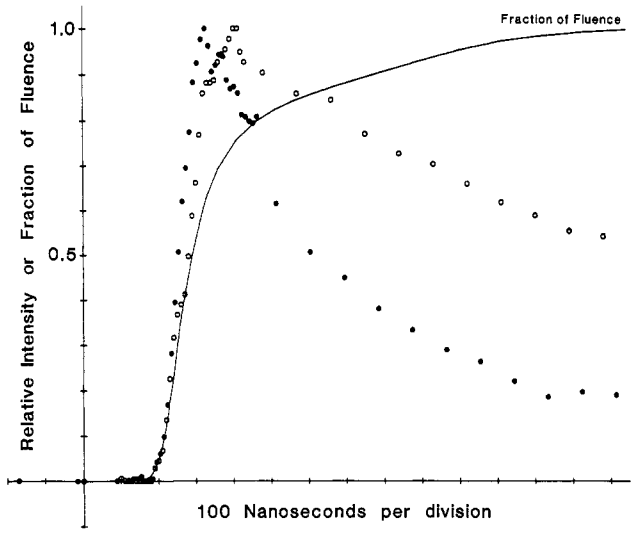

Figure 2. Fraction of 1023-cm^{-1} IR pulse fluence, and of luminescence at 360 (solid circles) and 560 (open circles) nm, plotted vs. time. Initial C_6F_6 pressure is 0.90 torr. The plasma shutter was not used in these experiments.

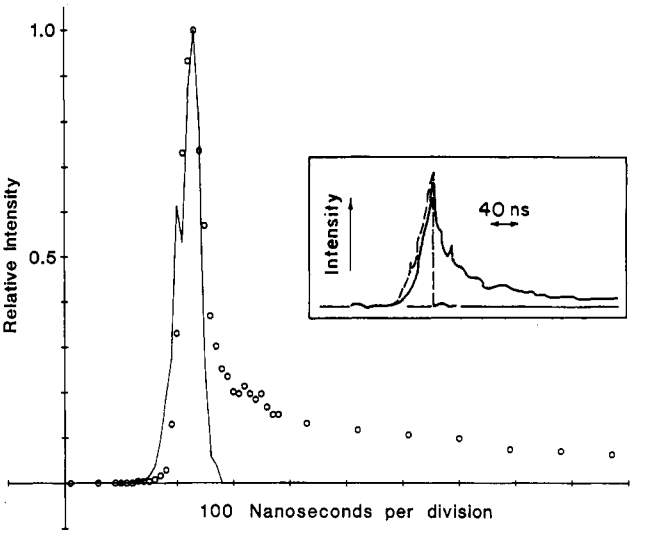

Figure 3. 1023-cm^{-1} truncated pulse intensity and luminescence at 360 nm (circles), plotted vs. time. Initial C_6F_6 pressure is 1.46 torr. Synchronization is accurate to within 20 ns. Overall system response time is ~20 ns. The insert shows a similar experiment recorded on the Tektronix storage oscilloscope with an overall system response time of ~10 ns.

300 times greater. If one risks extrapolating the absorption law to this intensity, one predicts that $dn_{abs}/dt = 2 \times 10^{10}$ s^{-1} and that $n_R = 110$, or 208 kcal mol^{-1} above threshold for C–F bond breaking.

In spite of uncertainty, it is clear that the reaction products are formed with large amounts of disposable energy, and that high temperatures can exist. For instance, a gas consisting entirely of C_6F_5 + F radicals, with a disposable energy of 140 kcal mol^{-1} per radical pair, at thermal equilibrium would be at 3000 K. It will be reported in a later section that the broad-background radiation emitted after the IR pulse indicates a temperature $^{\phi}T$ of 3500 K. In view of the preceding calculation, a temperature of that magnitude is credible.

Luminescence Kinetics. Using a 360- or 560-nm interference filter and nontruncated IR pulses of <500 J cm^{-2} fluence, one observes fast-rising and -decaying luminescence signals. Samples are shown in Figure 2, along with a synchronized plot of fraction of fluence vs. time. Although the luminescence begins shortly after the start of the IR pulse at both wavelengths, the kinetics of emission at later times becomes quite different.

In order to eliminate luminescence associated with continued IR pumping in the tail region of the IR pulse, a plasma shutter was built which truncated IR pulses after 60–80 ns. Figure 3 shows typical results obtained at 360 nm. The emission signal follows the rise of the IR intensity with an incubation period of <20 ns. On truncation of the IR pulse the emission decays. The kinetic plot of log emission vs. time (Figure 4) indicates two processes. About 8/10 of the signal at 1.46 torr decays quickly, with $\tau_A \approx$ 15 ns (determined within a factor of 2). The remainder decays with $\tau_B = 575 \pm 75$ ns. For experiments involving pure C_6F_6, τ_B is independent of pressure throughout the entire range, 0.145–1.46 torr. τ_A is independent of pressure between 0.8 and 1.7 torr.

Kinetic plots of emission accompanying *non*truncated IR pulses are similar to Figure 3, but there are quantitative differences. In particular, the plot of log emission vs. time, during the same time period in which τ_B was measured accurately after a truncated pulse, is now curved and the average slope is a weak function of pressure, increasing from 650 ns at 0.240 torr to 1400 ns at 3.07 torr. The comparison convincingly demonstrates the simplification in kinetic analysis made possible by IR pulse truncation.

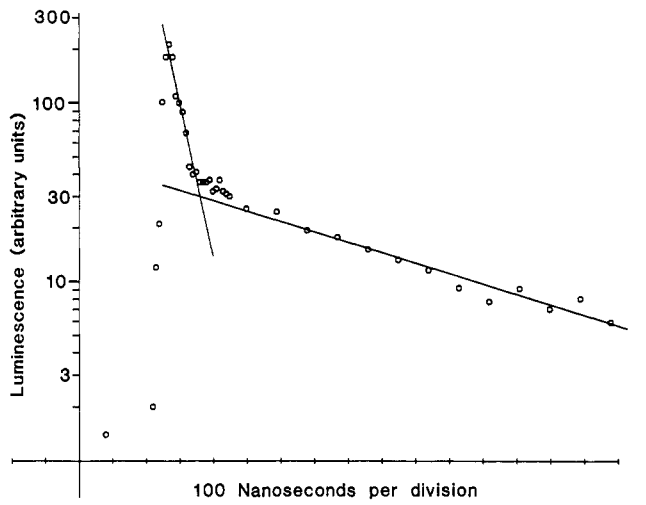

Figure 4. Log/normal plot of luminescence at 360 nm vs. time for data obtained under the same conditions as those in Figure 3.

Addition of 1.7 torr of O_2 to 1.7 torr of C_6F_6 increased the luminescence yield at 360 nm, reduced the fraction decaying with ~15-ns decay time, and gave a more curved plot of log emission vs. time, suggestive of the presence of new and/or more emitting species.

Addition of 2.0 torr of N_2 to 2.0 torr of C_6F_6 reduced the luminescence yield at 360 nm without reducing the fraction decaying with ~15-ns decay time.

Addition of 300 torr of Ar to 2.0 torr of C_6F_6 reduced the luminescence yield and practically eliminated the ~15-ns decay. Instead, >97% of the luminescence decayed with simple first-order kinetics and with $\tau = 440$ ns.

The kinetics of luminescence transmitted by the 560-nm interference filter differs considerably from that at 360 nm. A typical kinetic plot obtained with a nontruncated IR pulse is shown in Figure 5. There is little if any decay with either the ~15-ns (τ_A) or 575-ns (τ_B) mean time observed at 360 nm. Instead, τ for the initial mean life of decay is somewhat pressure dependent, increasing from 1.6 μs at 0.43 torr to 3.1 μs at 2.2 torr. τ for subsequent mean lives of decay tends to be longer; i.e., the kinetics is not pseudo first order. Kinetics plots are not noticeably different when the IR pulses are truncated after 60–80 ns.

TABLE I: Data for UV/Visible Emission Spectra

emission band	maximum, nm	fwhm, nm	τ,[a] ns	fine structure	ref
C_6F_6, $^1S_1 \rightarrow {}^1S_0$	360	70	<1-3 (L) 500 (R)	no	19
$C_6F_6^+$, $\tilde{B}(^2A_{2u}) \rightarrow \tilde{X}(^2E_{1g})$	462	40	48 ± 2 (L)	yes	20
CF_2 $\tilde{A}(^1B_1) \rightarrow \tilde{X}(^1A_1)$	296	40	61 ± 3 (R)	yes	21c
$^3B_1 \rightarrow \tilde{X}$	561	90		yes	21a
C_3 405-nm group	405	~6	200 ± 10[b] (L)	yes	23
violet continuum	400	60	$20g''/g'$[c] (R)	no	22
C_2 Swan bands					
$\Delta V_{em} = 0$	512	[d]	170 (L)	yes	5b
$\Delta V_{em} = -1$	466	[d]			
CF $\tilde{A} \rightarrow \tilde{X}$	234[e]		19 (L)	yes	5b

[a] L: luminescence. R: radiative. [b] Emitting state generated by (1) microwave discharge in C_2H_4 and (2) laser excitation of the resulting C_3. [c] Deduced from oscillator strength in absorption. Accuracy within a factor of 2. If the upper (g'') and lower (g') states are the same as for the 405-nm group, $g''/g' = 2$. [d] ~5 nm at 3000 K. [e] Zero-zero transition.

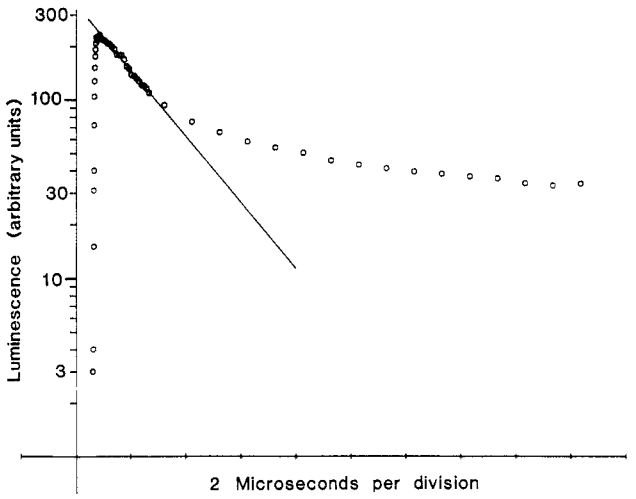

Figure 5. Log/normal plot of luminescence at 560 nm vs. time. Initial C_6F_6 pressure is 1.75 torr. Nontruncated IR pulse; see text.

Time-Resolved Luminescence Spectra. In the hope that some of the luminescing species might be identified, time-resolved emission spectra were taken in the 275–650-nm range. These spectra were rather coarse grained; in much of the range emission was measured only at 25-nm intervals, and some narrow bands may have been missed. Nontruncated IR pulses were used. However, the first time period comprises the initial 300 ns of the IR pulse during which 80% of the fluence is delivered. The next period of 500 ns and the subsequent period of 1 μs comprise the tail end of the IR pulse (16% and 4% of fluence, respectively) and are approximately after pulse. Subsequent periods are accurately after pulse.

The kinetic spectroscopy results had shown that at 360 nm there are luminescences with decay times τ_A ~15 ns and τ_B = 575 ± 75 ns. Figure 6 shows the luminescence spectrum emitted between 8.8 and 18.8 μs after the start of the IR pulse, when the decay of these emissions would be practically complete. This spectrum consists of a broad background, reproduced well by the blackbody radiation spectrum at $^\phi T$ = 3440 K, superimposed on which are statistically significant peaks at 512 ± 6, 466 ± 6, and 540 ± 6 nm. The peaks at 512 ± 6 and 466 ± 6 nm can be assigned to C_2 Swan bands with $\Delta V = 0$ and −1, respectively.[5b] That at 540 ± 6 nm is uncertain. Through an oversight, the Swan band with $\Delta V = +1$ around 560 nm was not measured.

Figure 7 shows the luminescence emitted *during and shortly after the pulse* in the 275–500-nm range. The broad background radiation, which is insignificant in much of this range, has been subtracted, as stated in the figure

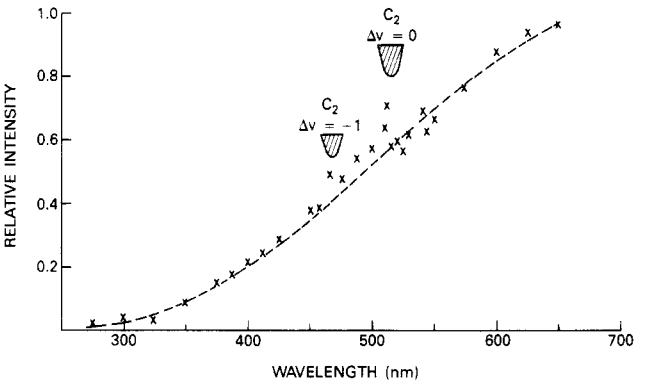

Figure 6. Luminescence spectrum, corrected for detection system wavelength response, emitted in the 8.8–18.8 μs interval, i.e., 8–18 μs after completion of the 1023-cm^{-1} IR pulse. The initial C_6F_6 pressure is 1.24 torr. Crosses: experimental points. Dashed curve: blackbody radiation at 3440 K. Shields: regions of C_2 Swan band emission.

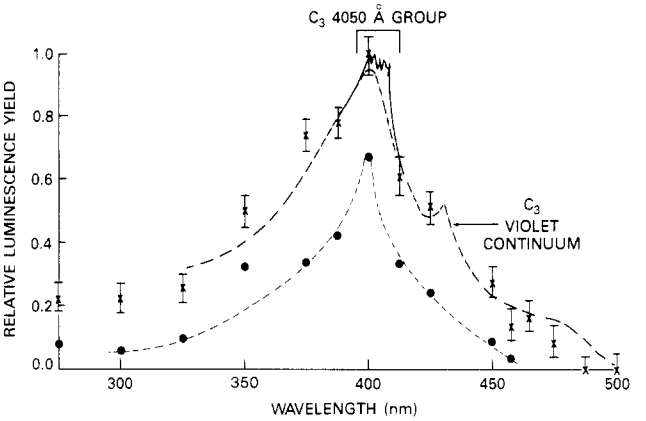

Figure 7. Luminescence spectrum, corrected for detection system wavelength response, emitted in the 0–0.3-μs interval (crosses) and in the 0.8–1.8-μs interval (solid circles). The initial C_6F_6 pressure is 1.24 torr. Broad-background radiation, taken to be blackbody radiation at 3440 K (as in Figure 6), has been subtracted; it was assumed that radiation emitted at 500 nm is 100% broad background. The upper dashed curve is a sketch of the C_3 violet continuum emitted by fuel-rich oxyacetylene flames at 2900 ± 200 K; the superposed solid curve includes the additional emission from the 4050-Å group.[22b,c] The lower dashed curve approximates the spectrum in the 0.8–1.8-μs interval.

caption. Table I summarizes a search of the literature for emission spectra of species that might be intermediates in the IR-induced decomposition of C_6F_6. The fluorescence emitted by the $^1S_1$ state of C_6F_6 gives a moderately close match, and intermediacy of $C_6F_6(^1S_1)$ would be of interest in connection with current theories of vibrational-to-

TABLE II: Time-Resolved Spectral Properties

interval, μs	spectral feature	integrated emission[a]	τ[b]	other
1st, 0–0.3	400-nm band	(1.000)		(Figure 7)
2nd, 0.3–0.8		0.830		
3rd, 0.8–1.8		0.511	590 ns[f]	
4th, 1.8–3.8	broad background	(1.000)[e]		ϕT = 3640 K
5th, 3.8–8.8		1.533	7 μs[g]	3470 K
6th, 8.8–18.8		2.007	17 μs[h]	3440 K
4th, 1.8–3.8	C_2 Swan bands	(1.000)[c]		1.87[d]
5th, 3.8–8.8		1.176	4.4 μs[g]	1.90[d]
6th, 8.8–18.8		0.793	6.5 μs[h]	1.86[d]

[a] Integrated emission over the wavelength range of the spectral feature and over the time interval. Initial $[C_6F_6]$ = 1.48 torr. [b] $\int_{t_j}^{t_k} I\,dt = (1 - A)/[A(1 - B)]$. $A = \exp([-t_j + t_i]/\tau)$; $B = \exp([-t_k + t_j]/\tau)$. [c] Measurements at 512 ± 6 and 466 ± 6 nm. Background radiation has been subtracted. [d] Luminescence at 512 nm/luminescence at 466 nm. Background radiation has been subtracted. [e] For the assumed blackbody spectra which fit the broad-background radiation. [f] 2nd/3rd interval. [g] 4th/5th interval. [h] 5th/6th interval.

electronic energy conversion.[24,25] However, the following facts argue against this assignment.

The absolute emission yield for the luminescence shown in Figure 7 was calculated by integrating the photon yield in the 325–425-nm range. Corrections were made for the broad-background emission and for system wavelength response. Assuming that emission comes only from the focal volume, we can then set an upper limit on the quantum yield (defined as number of photons emitted/number of C_6F_6 molecules initially in the focal volume). For the 0.0–0.3-μs measuring period during which $C_6F_6(^1S_1)$ emission might be present, this upper limit is on the order of 4×10^{-4}. As two of us have shown,[26,33] this quantum yield is markedly greater than the maximum that can plausibly be assigned to C_6F_6 fluorescence, so that the latter makes at most a small contribution to the emission reported in Figure 7. It should also be noted that the emission maximum in Figure 7 differs by 40 nm from that reported for UV-excited C_6F_6 (Table I).

On the other hand, the emission shown in Figure 7 gives a *good* match to emission in this range previously assigned to C_3.[22,23] Sketched in Figure 7 is the emission from fuel-rich oxyacetylene flames at 2900 ± 200 K, reported by Marr and Nichols,[22b] which consists of the 4050-Å group of C_3[23] and of a "violet-continuum" band that has also been ascribed to C_3.[22] Our experimental points for emission during the IR pulse bear a close resemblance to the violet-continuum band (our experiments give no information concerning 4050-Å-group emission), and the decay time τ_A of ~15 ns (uncertain by a factor of 2) is consistent with the radiative lifetime based on the oscillator strength of this band in absorption (Table I.)[22a]

Also shown in Figure 7 is the spectrum emitted from 0.8 to 1.8 μs after the start of the IR pulse. To a good approximation, this time interval occurs after both the IR pulse and the ~15-ns emission have decayed. Surprisingly, the 0.8–1.8-μs spectrum closely resembles the 0–0.3-μs spectrum emitted *during* the IR pulse. To be sure, the 0.8–1.8-μs spectrum is somewhat narrower, but its peak is at the same wavelength, 400 nm, as that of the 0–0.3-μs spectrum, and one might expect the temperature to be somewhat lower. To probe this matter further, Table II lists integrated emission yields for the band during two time intervals, 0.3–0.8 and 0.8–1.8 μs, both of which occur practically after the IR pulse. The data lead to an emission decay time of 590 ns in good agreement with the decay time τ_B = 575 ± 75 ns reported in the preceding section, so that the spectrum associated with τ_B is now characterized.

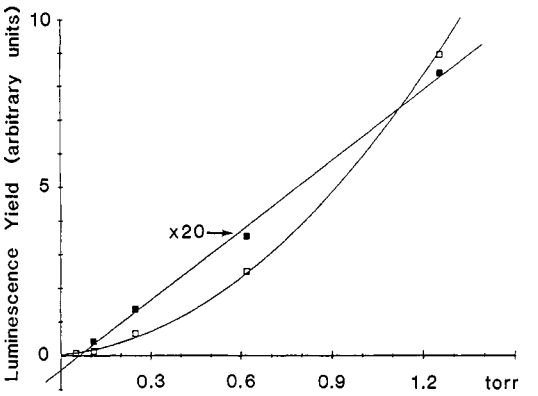

Figure 8. Luminescence yield as a function of initial pressure of C_6F_6. Constant IR pulses at 1023 cm^{-1} were used. Solid squares: observations in the 0–0.3-μs interval at 350 nm. Open squares: observations in the 3.8–18.8-μs interval at 512 nm. Straight line: linear least-squares fit of data at 350 nm. Conic section: quadratic least-squares fit of data at 512 nm.

If this is granted, then there are two interpretations. Either the similarity between the 0.8–1.8-μs spectrum and the violet-continuum band is fortuitous, or the spectrum is indeed the violet-continuum band, but then the discrepancy between the observed 575-ns decay time and the intrinsic ~15-ns radiative decay time of the emitting state must be explained. A straightforward kinetic explanation would involve the attainment, shortly after the IR pulse, of a dynamic steady state, i.e., secular equilibrium, as shown symbolically in eq 5.

$$A \xrightarrow[575\text{ ns after IR pulse}]{<15\text{ ns during IR pulse}} B^* \xrightarrow[\text{(spontaneous)}]{\sim 15\text{ ns}} B + h\nu \quad (5)$$

Our observations may have a bearing on recent discussions concerning the electronic spectroscopy of C_3—in particular, whether the 405-nm-group and violet-continuum emissions come from the same excited electronic state.[22a,23b] Since the luminescence lifetime of the 405-nm group has been found to be 200 ns,[23b] our results increase the weight of evidence in favor of the existence of two distinct excited electronic states of similar energy.

Formation of Luminescing Species. For C_6F_6 gas, at IR fluences up to 1 J cm^{-2}, it was found[18] that the relation of absorbed energy (E_{abs}/mol) to IR fluence in optically thin cells is independent of pressure. Because pressure-independent IR absorption is characteristic of molecules in their vibrational quasi-continua, we would expect E_{abs} to be at least approximately independent of pressure also in the present experiments. On that basis, measurements of luminescence yield as a function of pressure, in optically thin cells, using IR pulses of constant intensity profile and fluence, can give information about kinetic order in the

(33) Duignan, M. T.; Speiser, S. "Time-Resolved Vibrational Spectroscopy"; Atkinson, G. H., Ed.; Academic Press: New York, 1983.

creation of specific luminescences.

Figure 8 shows luminescence yield as a function of initial C_6F_6 pressure upon irradiation with constant IR pulses under two conditions: (1) At 350 nm during the first 0.3 μs after the start of the IR pulse, during which period most of the IR fluence is delivered. This experiment probes the time-resolved spectrum shown in Figure 7. (2) At 512 nm during the period from 3.8 to 18.8 μs after the start of the IR pulse. This period comes after completion of the IR pulse. The radiation whose creation is probed under these conditions is 80% broad background and 20% C_2 Swan band emission.

As shown in Figure 8, luminescence yield under condition 1 is nearly proportional to the initial C_6F_6 pressure. (The small negative intercept is within experimental error.) The luminescence yield under condition 2, on the other hand, shows an accurate quadratic dependence. Although these experiments give no information about kinetic order with respect to IR radiation density, we shall designate the linear plot as first-order kinetics, and the quadratic plot as second-order kinetics.

The detailed kinetic information derivable from the plots is limited. It is unlikely that such luminescing species as C_3 or C_2 are immediate decay products, formed from C_6F_6 in a single kinetic step. The observed kinetic orders therefore result from the convolution of kinetic orders in stepwise sequences. The simplest interpretation of the first-order result obtained under condition 1 at 350 nm is that the luminescing molecules are created during the period of intense IR irradiation in reaction channels consisting of unimolecular steps. Similarly, the second-order result obtained under condition 2 at 512 nm implies most simply that the luminescence, or the luminescing molecules, are created by a mechanism which involves a rate-determining bimolecular process in which the reactants or colliding molecules are derived from C_6F_6 in unimolecular steps.

In spite of the stated uncertainty, the *difference* in the kinetic results obtained under the two conditions strikes us as quite significant. Clearly there is a difference in mechanism of formation between the short-lived luminescing species present during and shortly after the IR pulse and the broad-background emission which becomes dominant after the IR pulse.

Apparent Temperatures. Table II lists the temperatures ${}^{\phi}T$ of the blackbody spectra which fit the broad-background radiation emitted during various time intervals after the IR pulse. Also listed are formal decay times τ (see note *b*, Table II) for the integrated broad background emission. It is worth noting that both the drop in ${}^{\phi}T$ and the decay of the emission are relatively slow. The nonconstancy of τ shows that the decay is not a first-order process.

In view of the appearance of a black solid among the final reaction products, the possibility exists that the broad-background radiation comes from colloidal particles suspended in the gas phase. At the prevailing pressures such particles would not form during a few microseconds after an IR pulse, so they would have formed after earlier pulses and been left in suspension. However, the following results indicate against this hypothesis.

The radiation emitted from a clean, freshly filled cell shows the same broad-background emission after the first IR pulse as after subsequent pulses, provided that the time between pulses is ~1 min or longer. Increasing the time between IR pulses has no effect. Reducing the time between IR pulses to well below 1 min causes an increases in background emission.

Consistent evidence for near-constancy of "temperature" during the observation period following an IR pulse comes from the Swan band emission of C_2. As shown in Table II, the C_2 luminescence at 512 nm ($\Delta V = 0$) and that at 466 nm ($\Delta V = -1$) are in a nearly constant ratio, showing that the vibrational temperature of the emitting electronic state of C_2 remains practically constant during the observation period. The resolving power of our monochromator does not permit an absolute evaluation of vibrational temperature, but a lower limit of >4000 K can be set. Notice however that the decay times for the C_2 emission are shorter than those for the broad-background emission, showing that the two processes are not connected by a steady-state equilibrium.

Concluding Remarks. This work was originally undertaken in the hope of finding $C_6F_6[{}^1S_1 \rightarrow {}^1S_0]$ fluorescence, but the results emphasize instead the dramatic speed with which even substances of high thermal stability such as C_6F_6 decompose into small fragments when a strong absorption band is irradiated at GW cm^{-2} intensities.

Although the luminescing species constitute only a small fraction of all the molecules in the irradiated gas, measurements of wavelength- and time-resolved luminescence are rewarding because results can be obtained, with relatively simple equipment, which indicate the chemical scope, kinetics, and effective temperatures. The present results characterize the emitting species only imperfectly, yet they suffice to indicate that chemical considerations must be different from those that pertain to reactions under less extreme conditions.

In particular, because of the high temperatures that exist during and shortly after the IR pulse, species which predominate during that time need not be closely related to the final reaction products. In the present experiments, the major gaseous product is C_2F_4. However, during the ~15-μs period following the IR pulse when effective temperatures approach or exceed 3500 K, C_2F_4 will be largely dissociated to $2CF_2$ ($K_p = [CF_2]^2/[C_2F_4] = 1.4 \times 10^7$ torr and $k_f \sim 10^9$ s^{-1} at 3500 K); CF_2 will be partly or largely dissociated to CF + F ($K_p' = [CF][F]/[CF_2] = 2.9 \times 10^2$ torr and $k_f' \sim 10^5$ s^{-1}), and the atomization of CF may also be significant ($K_p'' = [C][F]/[CF] = 9$ torr).[5a] It is only at later times after irradiation, when temperatures are lower and larger molecules are favored at equilibrium, that the nature of the final products is determined. In this view, the final reaction products indicate not how the parent molecules decompose but how the fragments formed from them upon GW cm^{-2} irradiation reassemble as the temperature returns to ambient under the given conditions.

Registry No. C_6F_6, 392-56-3; C_3, 12075-35-3; C_2, 12070-15-4; C_2F_4, 116-14-3.